ORIGINAL RESEARCH ARTICLE

Response patterns of phytoplankton growth to variations in resuspension in the German Bight revealed by daily MERIS data in 2003 and 2004[☆]

Jian Su [a,b,*], Tian Tian [c], Hajo Krasemann [a], Markus Schartau [a,d], Kai Wirtz [a]

[a] Institute of Coastal Research, Helmholtz-Zentrum Geesthacht, Geesthacht, Germany
[b] Institute of Oceanography, Centre for Marine and Climate Research, University of Hamburg, Hamburg, Germany
[c] Danish Meteorological Institute, Copenhagen, Denmark
[d] GEOMAR Helmholtz Centre for Ocean Research Kiel, Kiel, Germany

Summary   Chlorophyll (chl *a*) concentration in coastal seas exhibits variability on various spatial and temporal scales. Resuspension of particulate matter can somewhat limit algal growth, but can also enhance productivity because of the intrusion of nutrient-rich pore water from sediments or bottom water layers into the whole water column. This study investigates whether characteristic changes in net phytoplankton growth can be directly linked to resuspension events within the German Bight. Satellite-derived chl *a* were used to derive spatial patterns of net rates of chl *a* increase/decrease (NR) in 2003 and 2004. Spatial correlations between NR and mean water column irradiance were analysed. High correlations in space and time were found in most areas of the German Bight ($R^2 > 0.4$), suggesting a tight coupling between light availability and algal growth during spring. These correlations were reduced within a distinct zone in the transition between shallow coastal areas and deeper offshore waters. In summer and autumn, a mismatch was found between phytoplankton blooms (chl $a > 6$ mg m^{-3}) and spring-tidal induced resuspension events as indicated by bottom velocity, suggesting that there is no phytoplankton resuspension during spring tides. It is instead proposed here that frequent and recurrent spring-tidal resuspension events enhance algal growth by supplying remineralized

ELSEVIER | **Production and hosting by Elsevier**

nutrients. This hypothesis is corroborated by a lag correlation analysis between resuspension events and in-situ measured nutrient concentrations. This study outlines seasonally different patterns in phytoplankton productivity in response to variations in resuspension, which can serve as a reference for modelling coastal ecosystem dynamics.

1. Introduction

Coastal areas exhibit great variability in physical and biological processes, making it difficult to pinpoint spatio-temporal algal growth distribution patterns. In large part, this variability results from a complex interplay of sediment resuspension, phytoplankton growth, grazing, aggregation, and sinking of particulate matter. Primary factors controlling coastal phytoplankton distribution and growth include surface temperature, turbidity, river nutrient loads, and benthic and pelagic consumers, as well as tidal mixing (Loebl et al., 2009; Malone et al., 1983; Soetaert et al., 1994). These factors interfere with strong horizontal advection (Lucas et al., 1999).

Resuspension is a physical process that occurs when bottom shear stress is high enough to lift sediment particles (Wainright, 1990). Physical causes of resuspension include strong winds and tidal currents. In winter and spring, strong winds generate turbulent mixing. In shallow waters, turbulence not only retains suspended particles in the water column, but also detaches benthic material. Both processes increase the concentration of suspended particulate matter (SPM). SPM in turn negatively affects light availability for phytoplankton growth (Fig. 1, May et al., 2003; Wild-Allen et al., 2002). Wind-induced mixing has indeed been shown to determine effectively the spreading of algal spring blooms in coastal seas (Mei et al., 2010; Tian et al., 2009). In shallow coastal seas, strong tidal mixing also influences phytoplankton growth (Sharples et al., 2006). For instance, weakened mixing during neap tides favours stratification (Simpson et al., 1990). Results from harmonic analysis (von Storch and Zwiers, 2001) of satellite SPM images in the southern North Sea suggest pronounced spring-neap variations, thereby revealing how changes in tidal mixing govern the distribution of SPM (Pietrzak et al., 2011). In summer and autumn, tidal currents cause resuspension of benthic material, which can supply nutrients from sediment layers or bottom water layers to the water column (Fig. 1). These remineralized nutrients originate from the decomposition of organic matter that sank out of the water column and accumulated on the seabed shortly after the spring bloom (Ehrenhauss et al., 2004). Therefore, explaining the origin of bloom events in autumn is difficult because it involves reconciling two conflicting resuspension effects (high turbidity versus nutrient recycling) on phytoplankton growth (Fichez et al., 1992).

To date, the role of resuspension in coastal phytoplankton growth has rarely been addressed on a system scale. Previous studies of the effects of resuspension were based on laboratory work or on local in-situ measurements (Koschinsky et al., 2001; Sloth et al., 1996; Tengberg et al., 2003). Spatial extrapolations of local resuspension effects are limited because resuspension and phytoplankton growth have a strong mesoscale component (Gerritsen et al., 2001; Lou et al., 2000; Stanev et al., 2007). Satellite ocean colour data provide a unique tool for monitoring these effects. However, given spatio-temporal variations in bathymetry, atmospheric forcing, and hydrography, resolving how mixing, nutrient availability, and light availability promote phytoplankton blooms in shallow coastal regions remains a challenging task, especially when compared to simpler open ocean conditions (Lucas et al., 1998).

The German Bight (GB), located in the south-eastern portion of the North Sea, is a shallow area with average water depths of about 22 m (Fig. 2). In such shallow water, wind and tidal waves have an impact on the bottom, and resuspension has an impact on the water column. Our synoptic view of biophysical processes in the GB is gradually improving thanks to continuing in-situ measurements and
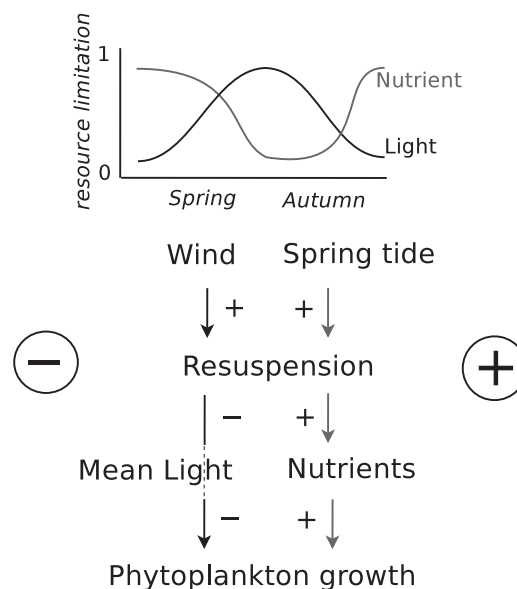
Figure 1 Schematic diagram of how resuspension influences phytoplankton growth. The upper graph generalizes the seasonal variations of the two main limiting factors in the German Bight: light and nutrients. The +/− signs with arrows indicate the positive/negative effects. In spring, phytoplankton reacts negatively to increased resuspension induced by wind. In contrast, in late summer and autumn, recurrent resuspension induced by the spring tide refuels phytoplankton growth with remineralized nutrients.

Figure 2 Topography (with 10, 20, and 30 m isobath) of the German Bight (left panel), which is located in the south-eastern North Sea (right panel). The black box in the left panel indicates the Helgoland area, for which a time series of MERIS data has been extracted. The area is centred on the Helgoland Roads long-term time-series station.
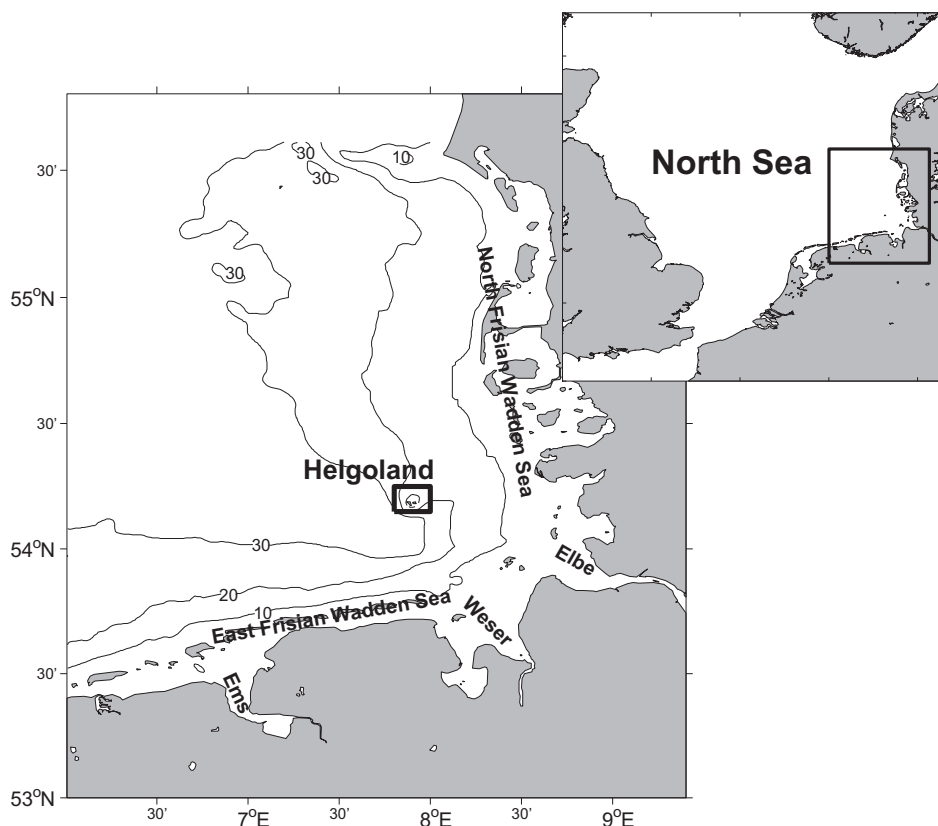
remotely sensed data (Grunwald et al., 2007; Onken and Riethmüller, 2010; Petersen et al., 2008; Staneva et al., 2009). Factors that limit phytoplankton growth in the GB are typical of shallow sea areas (Cloern, 1999; Colijn and Cadée, 2003). The primary limiting factor, as derived from the Helgoland Roads (HR) time-series data, is light limitation during spring blooms and nutrient limitation during summer and autumn blooms (Fig. A.1; detailed calculations are given in Appendix A).

This study has analysed remote-sensing data from the GB in 2003 and 2004 to unravel the interdependencies between algal growth and wind/tidal induced resuspension over space and time. The central question addressed in this paper is whether typical response patterns of spring or autumn algal blooms can be inferred from variations in resuspension. This study contributes to an improved quantitative and mechanistic description of direct coastal oceanographic effects on biogeochemistry and plankton ecology. Hence, it serves as a basis for multi-year studies and coupled physical—biological models.

2. Methods

2.1. MERIS derived products

The high-resolution satellite ocean colour images used in this study were obtained from the Medium Resolution Imaging Spectrometer (MERIS). MERIS provides high-resolution spectral data of water-leaving radiance for nine visible channels. These spectral data yield detailed information which is especially needed for case-2 waters (Bricaud et al., 1999). The North Sea was referred to as case-2 waters by Morel and Prieur (1977).

Maps of chl a concentrations are a standard MERIS product. Here, the version for case-2 coastal waters was used. The Case-2-Regional (C2R) processor in version 1.1 includes an atmospheric correction using bands in the infrared and blue spectral regions and a neural network to determine atmospheric contributions to the signal (Doerffer and Brock-mann, 2006). A comparison of C2R products with buoy data shows better agreement with water-leaving reflectances than that obtained from standard processors (Doerffer et al., 2010). The difference between in-situ and remote-sensing measurements, however, is highly dependent on patchiness, absolute concentrations, and the conversion from absorption lengths to concentrations. For case-1 waters, deviations are on the order of 10—30%; for chl a concentrations are above 0.5 mg m^{-3}. In-situ validations with case-2 waters are also very dependent on the region. For North Sea waters, pixel-wise differences are comparable to case-1 waters for high chl a and low suspended matter, but they can exceed the 100% level (Doerffer, 2007). The original 1 km resolution was not part of a regular grid, which poses difficulties for the analysis, and therefore for this study, a 2 km resolution was used. The reprocessed data included not only the standard output, such as chl a, chromophoric dissolved organic matter (CDOM) and total suspended matter (TSM) concentrations, but also the apparent optical

parameter for the attenuation coefficient K_d. In the North Sea, the observed Secchi depth (SD) shows a higher correlation with MERIS K_d in the transitional waters of the GB (R. Doerffer, pers. comm.). K_d fields will therefore be used in this study to approximate the spatial distribution of light attenuation coefficients, also motivated by Tian et al. (2009) who assimilated satellite-derived K_d to improve their model predictions for spring bloom events in the GB.

Because for 2003 and 2004 a relatively high number of cloud-free scenes could be processed, the present study concentrated on these years. Consequently, all subsequently integrated data were confined to these 2 years. MERIS chl *a* time-series at Helgoland were extracted by averaging chl *a* within the Helgoland area (indicated in Fig. 2).

2.2. Supporting model and time-series datasets

Time series of current velocity in the bottom layer and mixed layer depths were obtained from the model run described by Staneva et al. (2009), who used the three-dimensional General Estuarine Transport Model (GETM). GETM is a free-surface, baroclinic, hydrostatic model especially adapted to tidal flats and shallow waters (Burchard and Bolding, 2002). The model system is forced by 6-hourly ECMWF re-analysis data, hourly river run-off, and time-varying lateral boundary conditions of sea surface elevations (Staneva et al., 2009). Hence, the two major factors (tide and wind) considered in this paper are well described.

HR (54°11′18″N, 7°54′E) time series were used to validate the MERIS chl *a* data and to investigate the correlation between nutrients and chl *a* in summer and autumn. The samples for chl *a* measurement at HR were extracted from fluorescence data using an algal group analyser (Knefelkamp et al., 2007; Tian et al., 2011).

Sea-level data were collected at the HZG Langeoog pile (7°28′E, 53°43′N) station. Sea-level data were used to represent the spring and neap tidal cycle indices of the coastal GB.

2.3. Parameters to identify the photosynthesis—irradiance relationship

The daily irradiance averaged over the MLD (I_m, Einst m^{-2} d^{-1}) was calculated as:

$$I_m = \frac{I_0}{kz}[1 - \exp(-kz)], \tag{1}$$

where I_0 is the daily surface irradiance [Einst m^{-2} d^{-1}], k is the attenuation coefficient [m^{-1}], and z is the surface mixed layer depth [m]. I_0 was estimated from measurements of photosynthetically active radiation (PAR) at Helgoland (http://coast.hzg.de/data/helgo_rad.html), k from the MERIS derived K_d, and mixed layer depths z from 3D GETM results.

Net rates of chl *a* increase/decrease (NR, mg m^{-3} d^{-1}) were calculated according to:

$$NR_{chl,n} = \frac{chl_n - chl_0}{n}, \tag{2}$$

where chl_0 is the chl *a* concentration [mg m^{-3}] at the onset of the bloom and chl_n represents the chl *a* concentration at day n.

To estimate the spatial distribution of the NR—I_m correlation, the entire GB region was divided into smaller subregions of area 0.05° by 0.05°. By gradually increasing the size of each subregion, I_m was modified until the range of I_m in adjacent subregions reached a critical value of 5 Einst m^{-2} d^{-1}. Hence, all subregions contained a spectrum of light regimes. Furthermore, the correlation coefficient between I_m and NR was calculated in subregions of increased size to represent the correlations in each smaller subregion.

3. Results

3.1. Resuspension versus photosynthesis in winter—spring

MERIS and the in-situ HR time series depicted similar temporal changes in chl *a* concentrations during spring 2003 and 2004 (Figs. 3 and 4, upper panel). They showed a pronounced phytoplankton bloom at the end of March in 2003 and end of April in 2004, as indicated by the significant increase of chl *a*. The local agreement between these two independent time series generates enough confidence in the credibility of the satellite-derived data to reflect actual patterns in chl *a* concentration in space (one failed validation of MERIS data with HR time-series in 2005 was shown in Appendix B).

Three consecutive patterns of chl *a* (22 March, 3 April, and 13 April 2003 in Fig. 3a—c) illustrate the spatio-temporal development of the spring bloom. The bloom was initiated near the coast (mean water depth <10 m), from where filaments with elevated chl *a* concentrations spread into offshore regions (Fig. 3a and b). The development of filaments was more pronounced offshore of the North Frisian Islands than in the offshore region of the East Frisian Islands (Fig. 2). The latter region, however, was partly hidden by clouds. After 10 days, the initial coastal bloom progressed to the central parts of the GB (Fig. 3b and c). Eventually, elevated chl *a* concentrations became widespread over the entire central GB (Fig. 3c). At the same time, an extended patch with reduced chl *a* concentrations appeared in the deeper part of the German Bight (green colour in Fig. 3c). In 2004, MERIS and the in-situ HR time-series both showed a pronounced spring bloom from the end of April to the end of May (Fig. 4, upper panel). Three consecutive patterns of chl *a* (21 April, 26 April and 16 May, Fig. 4a—c) were selected to illustrate the development of the spring bloom. The general features of the development of the bloom were similar to 2003.

The timing of the spring bloom is mainly controlled by temporal differences in the amount of light penetrating through the water column. Turbidity measurements reveal sporadic changes in space and time in the GB. These variations are associated with resuspension of sediment particles. Coastal areas are highly turbid during the winter months. Likewise, on 22 March 2003, high turbidity was induced by strong resuspension, as seen in MERIS-derived TSM data (Fig. 5a). In a qualitative manner, the distribution of the average irradiance (I_m, Fig. 5b) was comparable to the distribution of TSM, because I_m is a function of the light-attenuation coefficient that is highly correlated with TSM. NR was calculated according to finite differences of chl *a*
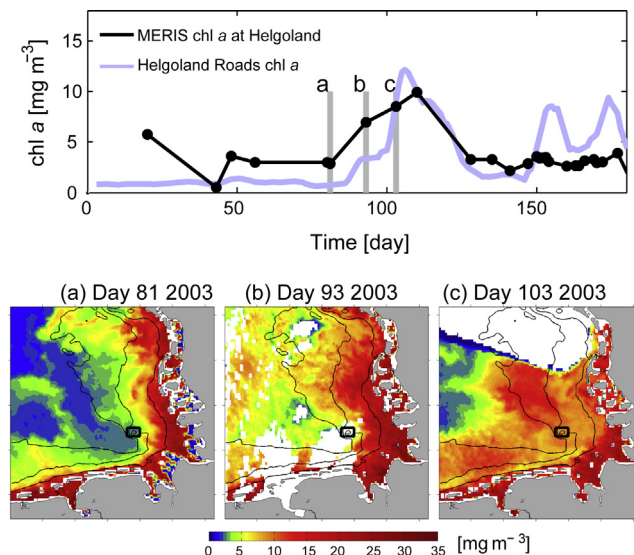
Figure 3 Upper panel: overlay of MERIS chl *a* time series at Helgoland (black line) and HR in-situ measured chl *a* time series (light purple line, cf. Tian et al., 2011) in 2003. The grey lines represent the dates of the three scenes shown in the lower panels, which display the development phases of a spring bloom. Lower panel: selected scenes of MERIS-derived chl *a* in the GB on (a) 22 March, (b) 3 April, and (c) 13 April 2003. The bathymetry of the GB is given by isobath lines. (For interpretation of the references to colour in this figure legend, the reader is referred to the web version of the article.)

between 22 March and 3 April 2003 and qualitatively matched the distribution of I_m (Fig. 5c). Substantial correlations between these three variables indicate a high sensitivity of phytoplankton growth to turbidity at the scale of the whole GB. To avoid repetitive descriptions, the maps of I_m and NR in 2004 were not shown here. I_m and NR in 2004 were calculated using two scenes from the initial phase of the spring bloom (21 and 26 April).

3.2. The sensitivity map of algal growth to limiting light

From Figs. 3 and 5, a qualitative picture of the spatial dependency between algal growth and light penetration could be obtained. To consolidate the interpretation, this correlation was quantified by calculating the spatial distribution of the NR-irradiance relationship in 2003 and 2004 (Fig. 6a and b).
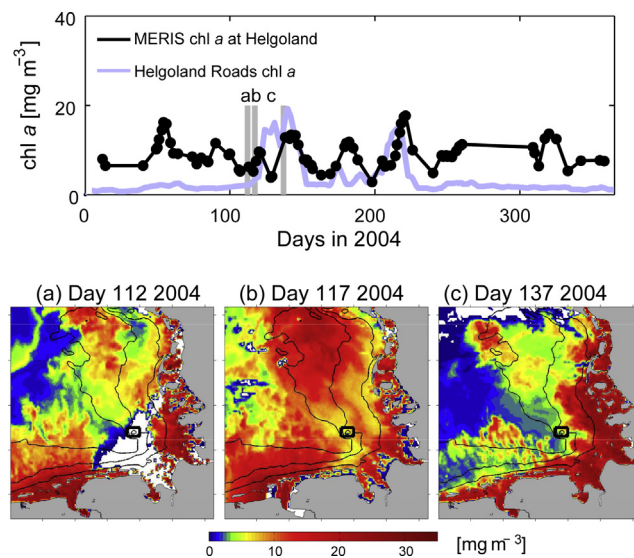

Figure 4 Upper panel: overlay of MERIS chl *a* time-series at Helgoland (black line) and HR in-situ measured chl *a* time series (light purple line) in 2004. The grey lines denote the dates of the three scenes shown in the lower panels, which display the development phase of a spring bloom in 2004. Lower panel: selected scenes of MERIS-derived chl *a* in the GB on (a) 21 April, (b) 26 April, and (c) 16 May 2004. The bathymetry of the GB is given by isobath lines. (For interpretation of the references to colour in this figure legend, the reader is referred to the web version of the article.)
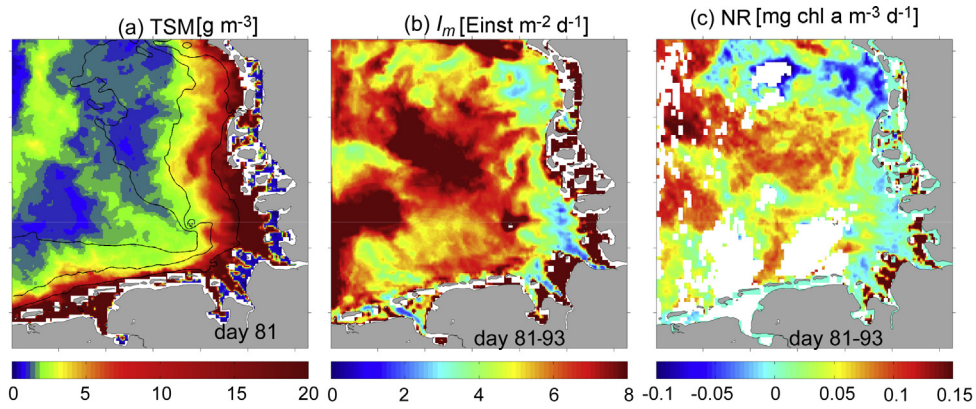
Figure 5 (a) MERIS-derived total suspended matter (TSM [g m^{-3}]) as a proxy for turbidity during the onset of the spring bloom, (b) mean water column irradiance within the mixed layer (I_m [Einst m^{-2} d^{-1}]) and (c) net rates of chl a increase/decrease (NR [mg chl a m^{-3} d^{-1}]). I_m is a function of K_d (day 81), mean PAR (days 81–93) and mean MLD (days 81–93). NR is calculated during the phytoplankton growth phase (days 81–93; see Fig. 3a and b).
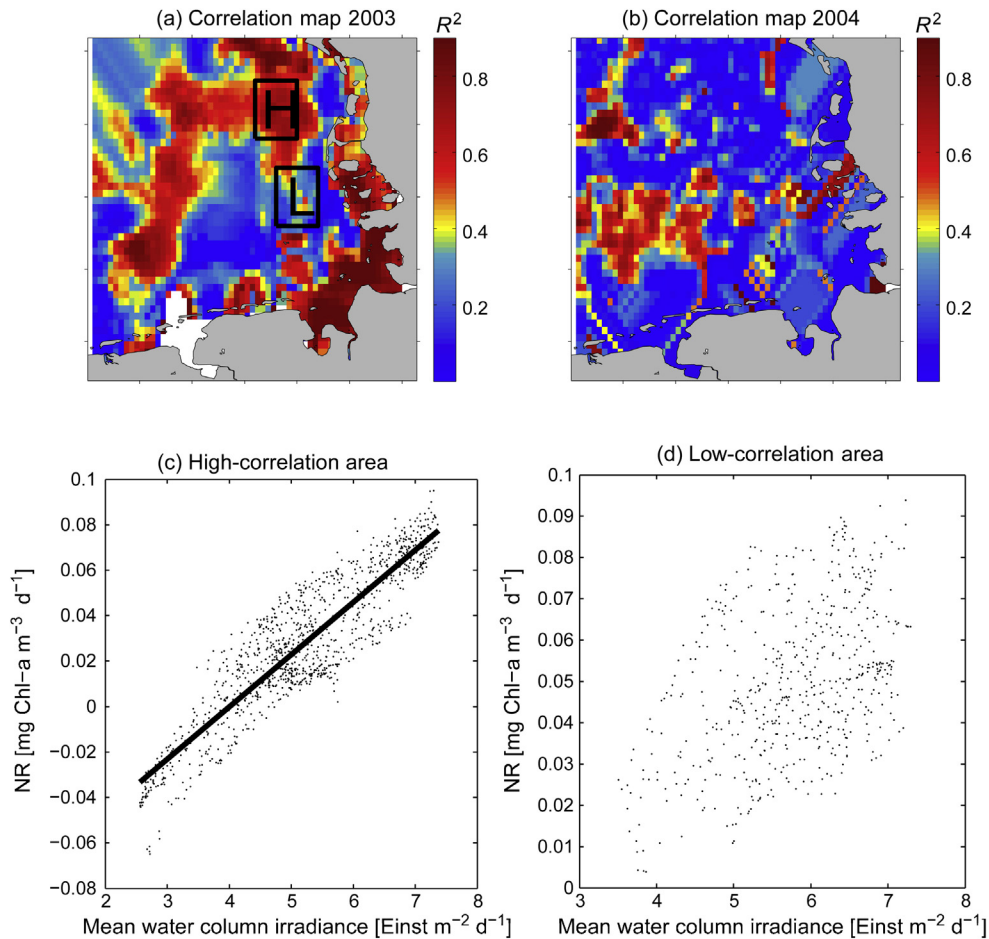
Figure 6 Upper panel: 2D map of the coefficient of determination R^2 between NR and I_m (Fig. 5b and c) in 2003 (a) and 2004 (b). Pixel resolution is 0.05°. The black boxes in (a) indicate two areas with high correlation and low correlation respectively. For these two boxes, scatter plots of NR and I_m are shown in bottom panels (c and d). In the high-correlation area ($R = 0.91$, $p < 0.001$), the illustration sheds light on the threshold of I_m to positive NR is 4 Einst m^{-2} d^{-1} (dashed lines). The slope of the NR-I_m relationship is denoted by α [mg chl a Einst^{-1} m^{-1}].

The correlation density distribution map showed that I_m and NR were highly correlated ($R^2 > 0.5$) in most regions in the central GB and within the coastal zone (depth <10 m, Fig. 6a). Regions with low correlation between I_m and NR formed a transition zone between coastal areas and the central GB, with depths between 10 m and 15 m. Over large areas, this transition zone coincided with the extended patch of decreased chl a concentrations along the coastal margin. The correlation map in 2004 illustrated a similar spatial pattern (Fig. 6b). To show examples of the relationship between I_m and NR in high- and low-correlation areas, scatter plots of I_m and NR are shown in 0.5° by 0.5° geographic boxes (Fig. 6c and d). Because NR is highly dependent on I_m in areas of high correlation (Fig. 6c), a positive NR was achieved when I_m exceeded 4 Einst m^{-2} d^{-1}. Scatters in low-correlation regions (Fig. 6d) suggested that factors other than light availability affected phytoplankton growth.

To quantify in more depth the relationship between algal growth and light in regions of high correlation, the slope of subregional NR—I_m regressions was estimated (α), which describes the sensitivity of algal growth to light (Fig. 7). The areas located on the offshore side of the Frisian Islands (black dots) and the Elbe Estuary (grey dots) showed a low slope ($\alpha < 12$ mg chl a Einst^{-1} m^{-1}) and also a limited variability in α with respect to the relatively high range of light availability (Fig. 7). In both regions, algal growth appeared to be insensitive to light because of highly turbid coastal waters. Moreover, a positive correlation existed between α and I_m on the offshore side of the Frisian Islands (black dots, $R = 0.29$, $p < 0.001$), indicating that algal growth could be sensitive to light if light conditions improved. In contrast, the range of α was large in the deeper GB (Fig. 7, blue dots).

The large variability in α may be due to strong variations in hydrographic conditions along with other possible factors, which will be discussed in Section 4.1.

3.3. Mismatch between strong resuspension events and the peaks of chl a in summer and autumn

Between April and October 2003 and 2004, the MERIS chl a time series at Helgoland revealed a series of recurrent bloom events after the spring blooms (Figs. 8d and 4). A bloom event (chl $a > 6$ mg m^{-3}) with cloud-free scenes on 13, 16, and 22 September 2003 was selected to study the chl a spatial pattern (Fig. 8a—c). This autumn bloom revealed spatially similar gradients from nearshore to offshore in large-scale pigment distribution, as was also observed during the spring bloom. Unfortunately, three cloud-free scenes could not be found in 2004 to show the development of the autumn blooms. Therefore, this analysis focusses on summer— autumn bloom dynamics in 2003.

In summer and autumn 2003, significant wind storms were absent in the GB, and repeated resuspension events were identified as induced by tides. Low-pass filtered, daily bottom current velocity (V_b) calculated by GETM exceeded the critical V_b for resuspension of 0.006 m s^{-1} in almost every bi-weekly spring phase (Fig. 9, Ziervogel and Bohling, 2003). The magnitude of the chl a peaks tended to increase in late autumn. Furthermore, all chl a peaks showed a timing mismatch with the resuspension events, indicating that chl a was not directly resuspended during the spring tide (e.g., from benthic diatoms).
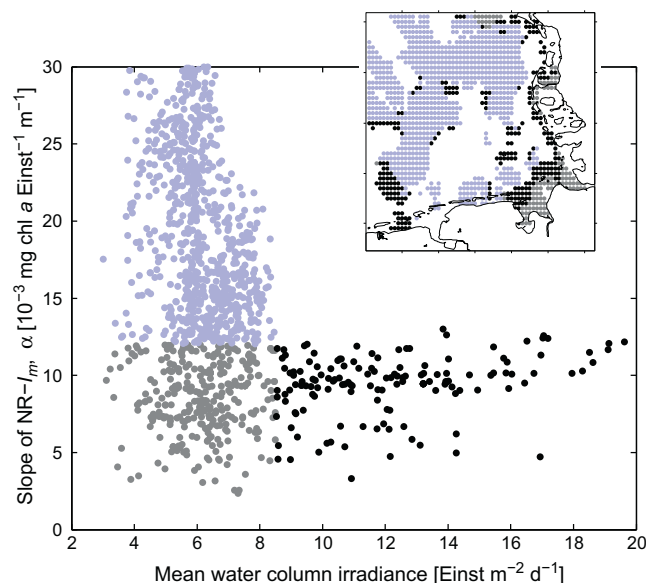

Figure 7 Relationship between mean water column irradiance (I_m) and the slope of the NR-I_m relationship (α). The analysis of tidal flat areas in the Wadden Sea was excluded because error signals were generated when the tidal flats ran dry. The dots represent MERIS-based observations of high I_m (black) and high α values (light purple), whereas the remaining part (where both α and I_m values are low) is plotted in grey. The black dotted areas exhibit a relatively low change range of α when I_m increases and are located on the offshore side of the Frisian Islands and the Elbe estuary (in the sub-figure). The blue pixels are located in offshore waters in the GB, which represent the area with a large change range in α and a small one in I_m. (For interpretation of the references to colour in this figure legend, the reader is referred to the web version of the article.)
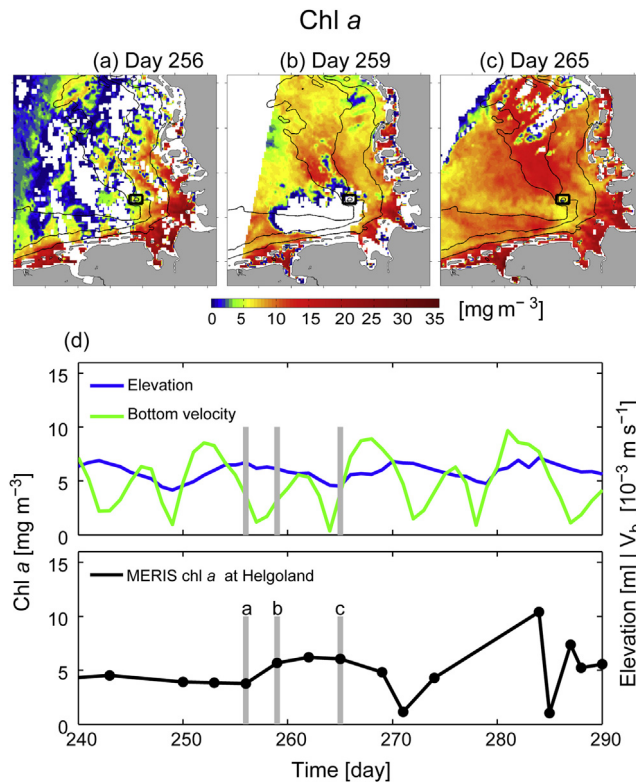
Figure 8 Selected scenes of MERIS-derived chl *a* in the GB on (a) 13 September, (b) 16 September, and (c) 22 September 2003, embracing a typical summer-autumn bloom event. (d) The temporal change of chl *a* in the lower panel is compared to tidal elevation and bottom current velocity in the upper panel. The tidal elevation is derived from Langeoog pile station time series, and the bottom current velocity is obtained from the model results at Helgoland.

In consideration of all these features, it was hypothesized that spring-tide induced resuspension imported nutrient-rich pore water from sediments or bottom water layers during spring tides during the nutrient limitation period, which gradually accumulated nutrients within the water column, eventually leading to phytoplankton blooms. Because nutrient measurements were spatially and temporally sparse, HR data were used to provide further verification of this hypothesis.
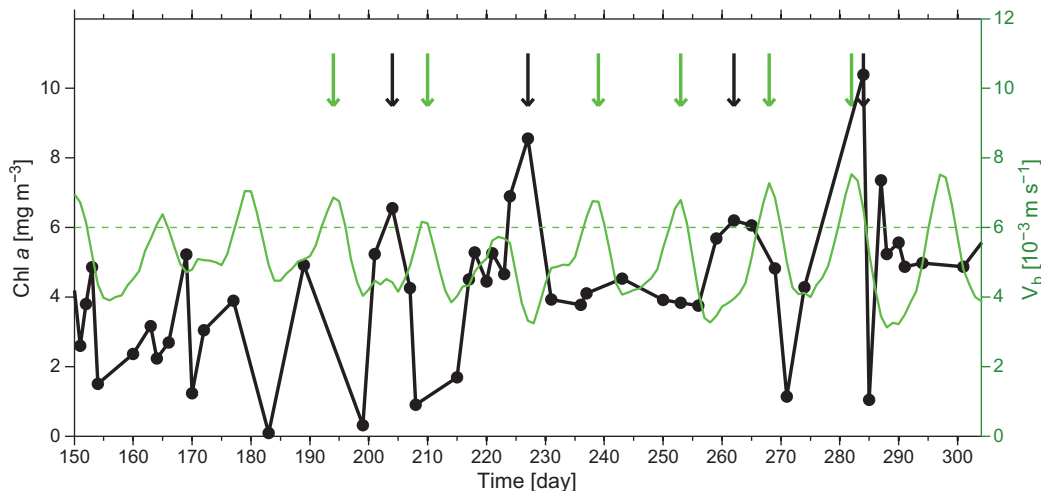
Figure 9 MERIS-derived chl *a* (black solid line) and bottom current velocity (green line, low-pass filtered) at Helgoland during summer and autumn in 2003. Resuspension events with the daily bottom velocity exceeding 0.006 m s^{-1} (over green dashed line) are indicated by green arrows. An autumn bloom is defined as an event when the chl *a* concentration exceeds 6 mg m^{-3}. Based on this bloom definition, where the chl *a* concentration should exceed 6 mg m^{-3}, four autumn bloom events were detected during late autumn (black arrows). (For interpretation of the references to colour in this figure legend, the reader is referred to the web version of the article.)

3.4. Time lag between resuspension and peaks of nutrients and chl *a*

If autumn blooms were triggered by a resuspended nutrient supply, there should be a delay between resuspension and the chl *a* peak due to the time needed to refill nutrient reserves in depleted phytoplankton cells and to achieve a massive build-up of biomass. Because the refilling processes of phosphate

and nitrate are different (as will be discussed in Section 4.2), a lag correlation analysis was used for both phosphate and nitrate. Analysis of in-situ measured phosphate at HR and resuspension intensity ($V_b > 0.006$ m s^{-1}) revealed a maximum correlation at no time lag in 2003 ($R = 0.51$, Fig. 10a) and at a 1-day lag in 2004 ($R = 0.46$, Fig. 10b), indicating that phosphate replenishment was directly accompanied by resuspension events. The lag correlation analysis for nitrate
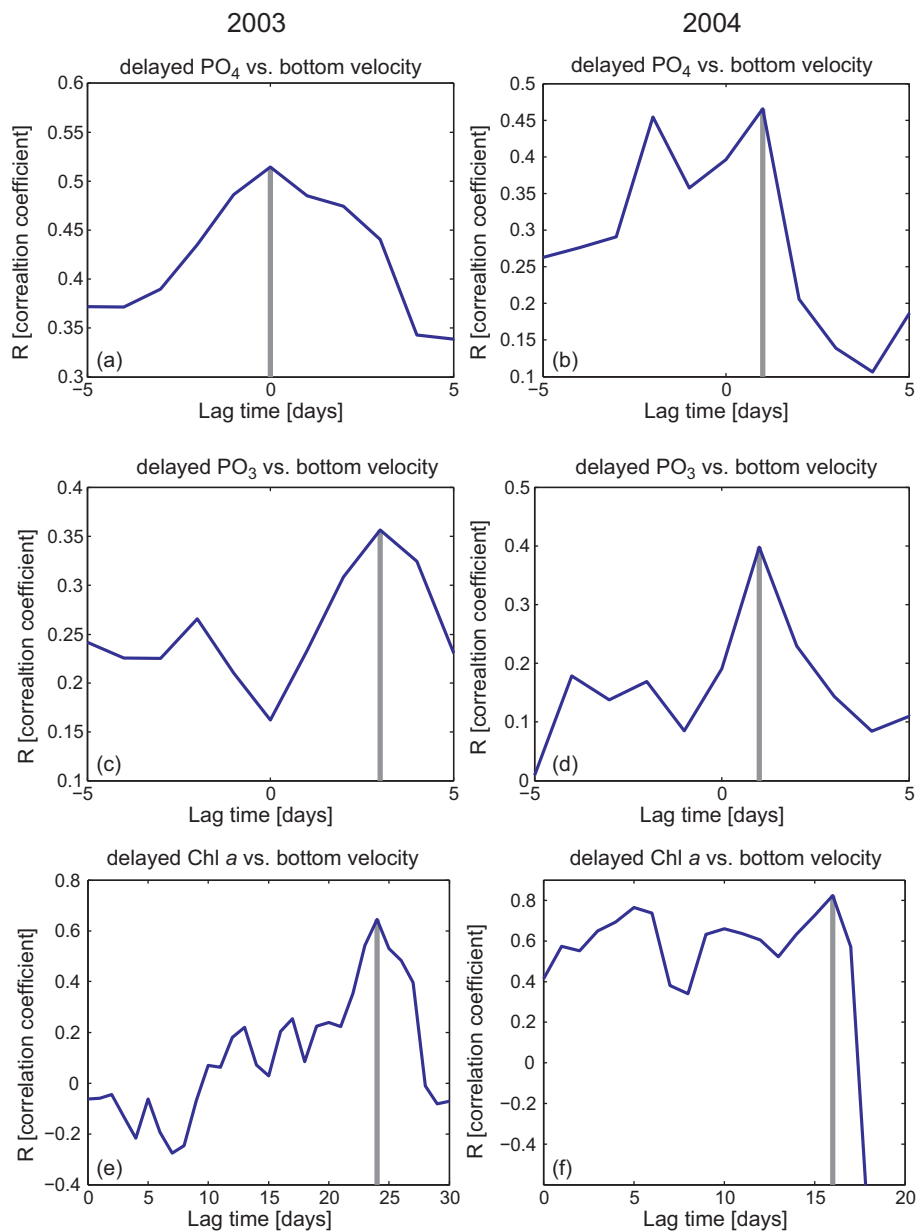

Figure 10   Lag correlations between HR in-situ measurements and bottom velocity which are greater than the critical threshold of 0.006 m s^{-1} (resuspension events) during summer and autumn (June—October) 2003 (left panel) and 2004 (right panel). (a and b) Correlations between lagged phosphate concentration [mmol m^{-3}] and simulated bottom velocity [m s^{-1}]. The grey line denotes the maximum of the correlation function at zero time lag in 2003 and a 1-day lag in 2004, indicating nutrient replenishment accompanied by tidal-induced resuspension ($R = 0.51$ in 2003, $R = 0.46$ in 2004, $p < 0.001$). (c and d) Correlation between lagged nitrate concentration [mmol m^{-3}] and simulated bottom velocity [m s^{-1}]. The grey line denotes the maximum of the correlation function at a lag of 3 days in 2003 and 1 day in 2004. (e and f) Correlation between lagged in-situ measured chl *a* [mg m^{-3}] and bottom velocity. The grey line denotes the maximum of the correlation function at a lag of 24 days ($R = 0.64$, $p < 0.001$) in 2003 and 17 days ($R = 0.8$, $p < 0.001$) in 2004, indicating that resuspension events preceded the chl *a* peak by this amount of time.

showed a maximum correlation at a 3-day time lag in 2003 and at a 1-day lag in 2004, with relatively lower correlations ($R < 0.4$, Fig. 10c and d).

The same lag correlation analysis (with the lag time extended to ± 30 days) between chl a peak and V_b showed that resuspension preceded blooms by 24 days in 2003 ($R = 0.64$, Fig. 10e) and by 17 days in 2004 ($R = 0.8$, Fig. 10f). This time lag could be the time needed for phytoplankton to build up biomass or a physiological response to nutrients. Nevertheless, the existence of a time lag already partially explains the mismatch between resuspension events and chl a peaks, as apparent in the MERIS data in Fig. 9, and therefore the number of days of delay should be interpreted with caution.

4. Discussion

The combination of in-situ measurements, satellite data, and model results provides a framework for iterative integration and assessment of spatial and temporal variability of phytoplankton production in the GB. Previous studies have already addressed bloom dynamics in the GB, but most of these have been limited by coarse spatial and temporal resolution (Colijn et al., 1990; Joint and Pomroy, 1993; Stoeck and Kroncke, 2001; Sündermann et al., 1999). Although the implementable MERIS data for the GB were restricted to days with little to no cloud cover, these data were sufficient to resolve extensive filament formation and to reveal details on patches that emerged in the course of phytoplankton bloom. Specification of these details supported model development, pinpointing spatial variations that need to be resolved by studies aimed at quantifying coastal primary production on a larger scale. The results obtained here support the establishment of causal links between turbulent mixing, resuspension, and phytoplankton growth on shorter time scales.

4.1. Resuspension as a negative factor: light attenuation and photosynthesis

The hydrodynamics of the GB are extensively forced by wind (Becker et al., 1999) and strong tidal currents (>1 m s^{-1}, Staneva et al., 2009). This forcing can generate high kinetic-energy dissipation, inducing small- to large-scale erosion of bottom sediments (Gayer et al., 2006). Local differences in sediment composition, with varying silt and sand contents, contribute to the variability apparent in strong temporal and lateral gradients in suspended-matter content (Becker et al., 1992, 1999). Reduced SPM has already been shown to act as a primary trigger for the phytoplankton spring bloom throughout the GB (Tian et al., 2009). In a multi-year spring bloom study in the GB, Tian et al. (2011) found that the spring bloom was preceded by a period of high wind speeds and developed only as the wind slackened.

In the present study, major parts of the GB in spring have revealed a high correlation between turbidity-related mean light levels and net rates of chl a increase/decrease (Fig. 6a). In such regions, chl a increments can therefore serve as an unequivocal proxy for phytoplankton growth. Because mean light levels depend mostly on local resuspension, high correlations indicate the important role of variations in turbulent

shear stress in bloom onset. Variations in turbulent shear stress depend on the tidal phase, but are dominated by storm events, which are most frequent in winter and spring. Bottom shear stress is particularly enhanced when strong winds act against the mean current direction (Staneva et al., 2009).

In contrast to areas with a clear growth—light relationship (in analogy to in vitro measurements of photosynthesis rates at varying PAR), central regions within the GB at intermediate water depths between 20 m and 30 m and located off the East Frisian Islands do not sustain a linear growth response to light enhancement (Fig. 6a). Whether these areas are subject to extensive grazing cannot be assessed due to the scarcity of measurements available for 2003. Massive grazing by zooplankton would compromise estimates of algal growth obtained from temporal changes in chl a concentration. In 2004, however, no horizontal gradients in abundance of mesozooplankton consumers were observed before or during the bloom phase (Renz et al., 2008). Therefore, in 2004, grazing pressure could not explain the observed pattern separation (high values in zones of low growth—light correlation). Nevertheless, although the 2003 evidence is inconclusive, grazing pressure is still a possible candidate to explain the pattern separation observed in 2003.

Other possible reasons for moderate to low growth—light correlation can be associated with mediocre data quality and with temporally strong loss factors like sedimentation, wind mixing (Koseff et al., 1993), or river runoff (Radach et al., 1990). These errors, however, should contribute to spatial heterogeneity, producing more scattered patterns in correlation intensity than were observed in this study.

4.2. Resuspension as a positive factor: nutrient enrichment and lagged growth response

Analysis of satellite images shows that the spring-neap tidal mixing (fortnightly tidal cycle) controls near-surface SPM concentration in the southern North Sea (Pietrzak et al., 2011). Spring-neap modulation of tidal mixing can have significant effects on the timing and magnitude of phytoplankton growth (Cloern, 1991; Sharples, 2008). In spring, the spring-neap tidal cycle regulates stratification, which may affect the timing of spring blooms. However, it was not possible to gather enough cloud-free scenes during this period to prove this point. Consequently, the focus shifted to the summer—autumn period, when nutrient limitation prevails in the system (Fig. A.1). Of course, light could also be a limiting factor during certain months in summer and autumn (e.g., September 2003, Fig. A.1). However, it could be a candidate only to explain the missing correlation between resuspension and nutrient replenishment (here it is referred to as a secondary factor).

Was the summer—autumn chl a periodicity due to directly resuspended subsurface chlorophyll? Balch (1981) found that in summer, diatom blooms off Monhegan Island always occurred at spring tides, possibly because of increased nutrients or the upward movement of a subsurface chlorophyll maximum layer. In studies of time-series chl a data off the Connemara coast, Ireland, Roden (1994) reported chlorophyll peaks occurring at neap tides in late summer. He argued that the driving mechanism was a localized accumulation of flagellates under stable neap-tide conditions. However, we

found no increase in chl *a* immediately following the spring tide and no clear match between phytoplankton blooms and neap tides (Fig. 9). Instead, a clear mismatch between the spring tide and the peak of chl *a* was observed, indicating that resuspended chlorophyll cannot be a candidate for explaining the summer—autumn chl *a* periodicity in the GB.

Sournia et al. (1987) recorded some variability in nutrient concentrations associated with spring tides, but variations in chl *a* did not appear to be associated with the spring-neap cycle in the western English Channel, which is strongly influenced by tides. This finding supports the hypothesis that resuspension events associated with spring tides refuel remineralized nutrients from sediments or the bottom water layer (Fig. 10a). These benthic nitrate fluxes depend on denitrification in the sediments (Hall et al., 1996; Wainright, 1990), and therefore spring tides refuel nitrate from sediments. This could explain why nitrate replenishment showed a relative low correlation with resuspension events (Fig. 10c and d). The phosphate data from the ICES dataset in the GB showed a gradually increasing trend in summer and autumn (Fig. A.1). Resuspension events can stimulate phosphate transport from the bottom water layer to the whole water column. However, the time lag between resuspension events and phytoplankton growth needs to be further discussed (Fig. 10b). This delay is the result of net phytoplankton growth, which is determined by the plankton community structure or by the physiological states of the algae. Related model studies, like that of Wirtz and Pahlow (2010), have shown that in addition to the time needed to build up biomass within an exponential growth phase, phytoplankton populations often need to acclimate their physiology (and their internal stoichiometry) to novel nutrient conditions, which can take up to several days. In fact, a distinct response pattern in phytoplankton growth was observed after the spring tide, at times when the bottom velocity exceeded critical values of 0.006 m s^{-1}. The response signal, however, was delayed by a few weeks. Chl *a* concentrations gradually increased with the onset of the neap tidal period, and a short-term maximum was reached approximately 10 days after the spring-tide resuspension event (Fig. 9). The repetition of this temporal pattern in autumn therefore reflects the modulation of two time scales, the spring tide cycle and the net algal growth rate of phytoplankton. Anomalies seen in this temporal pattern must be attributed to secondary factors that could not be further specified here.

4.3. Limitations of remote-sensing data

To characterize intermediate-scale chl *a* variability, it was a methodological prerequisite to rely on data accuracy and data with sufficient temporal resolution. In a previous remote-sensing study of the North Sea, Henderson and Steele (1993) encountered problems in interpreting sub-mesoscale (1—10 km) plankton dynamics using satellite chl *a* data stemming from the Coastal Zone Colour Scanner (CZCS, 1978—1986). With more modern instruments like MERIS, the sensitivity and the signal-to-noise ratio are significantly increased. Recent reports (Doerffer et al., 2010) showed systematic differences of less than 10% between in-situ and satellite-measured water-leaving reflectance. The

frequency of scenes, 2 out of 3 days, is limited and must be further reduced to a usable value of once every 3 days (Müller et al., 2015). This remains a critical factor when resolving temporal changes that coincide with time-series data (e.g., Figs. 6 and 9). In addition, the systematic errors of satellite-derived data show periodic features, which are not yet fully understood, but most likely result from illuminating and observing geometries and are frequencies related to revisits under similar geometrical conditions (Müller, 2010).

This variability should also be interpreted carefully for other reasons. Satellite-derived chl *a* estimates in highly turbid water are still subject to significant uncertainties. A mismatch was also found between MERIS data and in-situ HR time series in 2005 (Fig. B.1). Moreover, in applications of SeaWiFS, chl *a*, concentration was considerably overestimated for the Bay of Biscay when SPM optically dominated the backscatter (Gohin et al., 2005). Although accuracy has been much improved by increasing MERIS spectral resolution and using more elaborate (neural network) algorithms, the presence of a remaining bias in the simultaneous determination of TSM, CDOM, and chl *a* cannot be fully excluded. In fact, TSM, CDOM, and chl *a* can be simultaneously determined with optimal accuracy only as long as they are equally prominent. If one of the components becomes the dominant error on the retrieval for the other components, this error increases significantly and can reach several hundred per cent in extreme cases such as estuarine turbidity zones. Because the present analysis was based mainly on a single measurement source, the true independence of the data compared cannot be assumed.

5. Conclusions

In spring 2003 and 2004, spatial patterns of phytoplankton production were well described using satellite-derived light-attenuation data within most coastal areas and the deeper open waters of the GB. This analysis was supported by good correlations between phytoplankton net algal growth rates and light availability. Weak correlations prevailed only within a distinctive zone (the coastal margin), which represents the transition between shallow well-mixed coastal waters and the off-shore area. Phytoplankton within this transitional zone was found to be particularly sensitive to SPM resuspended from the seabed or from near-bottom water layers. Because of opposing responses in algal growth to resuspension, phytoplankton growth becomes difficult to estimate during post-bloom periods in summer and autumn. A mismatch between distinct phytoplankton blooms and tidally induced resuspension events indicates that phytoplankton resuspension plays a limited role during spring tides. Resuspension-imported nutrient-rich water from sediments or bottom water layers, however, did stimulate time-lagged phytoplankton growth responses.

In summary, typical spring and summer—autumn bloom patterns can be inferred on regional scales. Phytoplankton growth co-varies with resuspension in both positive and negative directions: positively in summer—autumn, and negatively in winter—spring, as summarized in Fig. 1. Now that regions where phytoplankton responds differently to variations in physical forcing have been identified, it will be possible to describe these processes better in biogeochemical and

ecological models to generate better explanations (or predictions) of event-scale phytoplankton blooms.

Appendix A. Limiting factors

The limiting factors on phytoplankton growth were reconstructed according to Cloern (1999). He developed a simple index to determine the relative importance of light and nutrient limitation for phytoplankton growth. Colijn and Cadée (2003) used this index to study the eutrophication problem in the Wadden Sea and found that the light limitation far exceeded the effects of nutrient limitation. Loebl et al. (2008) followed this approach and showed increasing nitrogen limitation during summer in the northern Wadden Sea. These applications of this approach revealed that this index is suitable for turbid coastal waters like the German Bight.

To investigate seasonal changes in the limiting factors on phytoplankton growth, this index was applied based on the Helgoland Roads time series of 2003 (Wiltshire et al., 2008). To calculate irradiance (I'), photosynthesis available irradiance (PAR) and Secchi depth data were used. The calculation of nutrient-limiting resources (N') was based on phosphate data, and K_{PO_4} was set to 0.5 in accordance with Moll (1998). The indices were illustrated with monthly mean data.

The detailed equations can be found in Cloern (1999). Using I' and N', a contour plot of the ratio of growth rate sensitivity to light and nutrients (R, Fig. A.1) was generated. The criteria used in Cloern (1999) were used to interpret the resource limitation map, where $R > 10$ was defined as a strong light limitation, $R < 0.1$ as a strong nutrient limitation, and $0.1 < R < 10$ as a joint limitation of light and nutrients.

In Fig. A.1, the light limitation was dominant in January and February ($R > 10$) until the spring bloom started in March ($R \approx 1$) in 2003, because high SPM concentration constrained phytoplankton growth before the spring bloom (Tian et al., 2009). Light was the factor triggering the spring bloom. From May to August, the GB was under a nutrient limitation ($R < 0.1$). Therefore, remineralization combined with tidal mixing could be important for triggering the summer—autumn blooms in terms of placing R between 0.1 and 10. The resource limitation map supplied the background information for the hypothesis of this paper and finally supported the authors concept.

To describe the re-mineralization processes in summer and autumn, nutrient data (especially for phosphate) are needed. However, nutrient measurements were spatially and temporally sparse. Phosphate data were obtained from an ICES nutrient dataset (http://ecosystemdata.ices.dk/). Phosphate data were also measured using surface bottle samples taken during cruises close to the Elbe Estuary (Fig. A.1 map). These nutrient data were used to construct the resource limitation map (Fig. A.1 diamonds). The indices showed that the nutrients started to refuel by the end of June. By mid-August, nutrients had already ceased to be a limiting factor, while the wind was still not very strong (unpublished wind data from Helgoland Roads). A gradually increasing trend in the summer and autumn period suggested that tidal mixing could be a candidate other than wind mixing for refuelling nutrients.
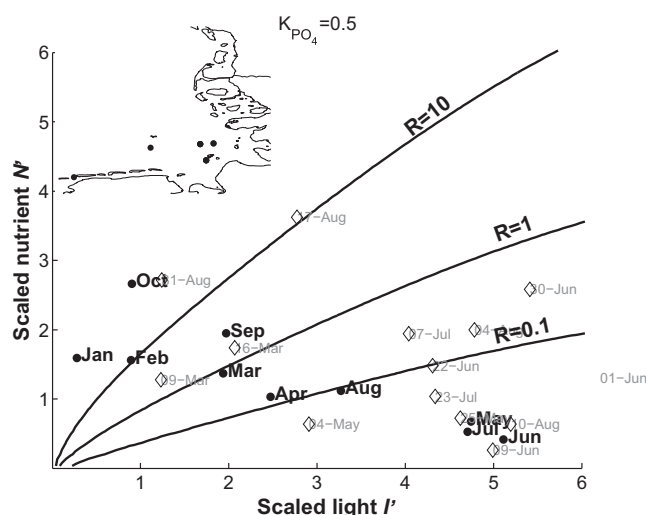

Figure A.1 Resource limitation map following the approach described in Cloern (1999) (for a detailed calculation, see Appendix A). Helgoland Roads Photosynthesis Available Radiance (PAR) and nutrient data were used to calculate the monthly index ($K_{PO_4} = 0.5$ according to Moll (1998)), which is represented by the black dots. The diamonds represent the indices calculated from the ICES nutrient dataset. The map in the upper left panel shows the locations (black dots) of the in-situ measurements. I' is the light limitation factor, and N' is the nutrient limitation factor. The area of $R > 10$ indicates strong light limitation, the area of $R < 0.1$ indicates strong nutrient limitation, and the area of $0.1 < R < 10$ indicates a joint limitation of light and nutrients.

Appendix B. Comparison of MERIS data with HR time series data in 2005

In 2005 MERIS and the in-situ HR time-series did not match very well, and it was not possible to find clear scenes to show the development of the spring bloom (Fig. B.1). Because atmospheric conditions vary from year to year, obtaining reliable long-term satellite data is still challenging (Müller et al., 2015). Therefore, validation of MERIS data in-situ measurements is necessary when using multi-year satellite data.
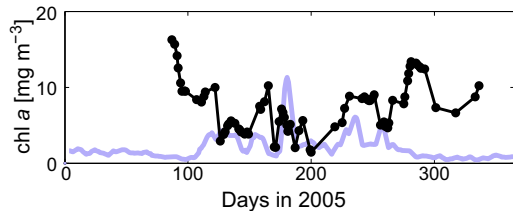

Figure B.1   Overlay of MERIS chl *a* time-series at Helgoland (black line) and HR in-situ measured chl *a* time series (light purple line) in 2005. (For interpretation of the references to colour in this figure legend, the reader is referred to the web version of the article.)

References

Balch, W.M.K., 1981. An apparent lunar tidal cycle of phytoplankton blooming and community succession in the Gulf of Maine. J. Exp. Mar. Biol. Ecol. 55 (1), 65—77.

Becker, G.A., Dick, S., Dippner, J.W., 1992. Hydrography of the German Bight. Mar. Ecol. Progr. Ser. 91 (1—3), 9—18.

Becker, G.A., Giese, H., Isert, K., König, P., Langenberg, H., Pohlmann, T., Schrum, C., 1999. Mesoscale structures, fluxes, and water mass variability in the German Bight as exemplified in the KUSTOS-experiments and numerical models. Ocean Dyn. 51 (2/3), 155—179.

Bricaud, A., Morel, A., Barale, V., 1999. MERIS potential for ocean colour studies in the open ocean. Int. J. Remote Sens. 20 (9), 1757—1769.

Burchard, H., Bolding, K., 2002. GETM — a general estuarine transport model. Scientific Documentation Tech. Rep. EUR 20253 EN European Commission. 157 pp.

Cloern, J., 1991. Tidal stirring and phytoplankton bloom dynamics in an estuary. J. Mar. Res. 49 (1), 203—221.

Cloern, J., 1999. The relative importance of light and nutrient limitation of phytoplankton growth: a simple index of coastal ecosystem sensitivity to nutrient enrichment. Aquat. Ecol. 33 (1), 3—15.

Colijn, F., Cadée, G., 2003. Is phytoplankton growth in the Wadden Sea light or nitrogen limited? J. Sea Res. 49 (2), 83—93.

Colijn, F., Villerius, L., Rademaker, M., Hammer, K., Eberlein, K., 1990. Changes in spatial distribution of primary production, photosynthetic pigments, and phytoplankton species composition during two surveys in the German Bight. J. Sea Res. 25 (1—2), 155—164.

Doerffer, R., 2007. The Meris Case 2 water algorithm. Int. J. Remote Sens. 28 (3), 517—535.

Doerffer, R., Brockmann, C., 2006. MERIS Case 2 Regional Processor User Manual, Version 1.1, http://www.brockmann-consult.de/beam/plugins.html.

Doerffer, R., Fischer, J., Preusker, R., Brockmann, C., Danne, O., 2010. Atmosphere and glint correction processor. Tech. Rep. ESA Contract No. 20598/07/I-O.

Ehrenhauss, S., Witte, U., Janssen, F., Huettel, M., 2004. Decomposition of diatoms and nutrient dynamics in permeable North Sea sediments. Cont. Shelf Res. 24 (6), 721—737.

Fichez, R., Jickells, T., Edmunds, H., 1992. Algal blooms in high turbidity, a result of the conflicting consequences of turbulence on nutrient cycling in a shallow water estuary. Estuar. Coast. Shelf Sci. 35 (6), 577—592.

Gayer, G., Dick, S., Pleskachevsky, A., Rosenthal, W., 2006. Numerical modelling of suspended matter transport in the North Sea. Ocean Dyn. 56 (1), 62—77.

Gerritsen, H., Boon, J.G., van der Kaaij, T., Vos, R.J., 2001. Integrated modelling of suspended matter in the North Sea. Estuar. Coast. Shelf Sci. 53 (4), 581—594.

Gohin, F., Loyer, S., Lunven, M., Labry, C., Froidefond, J., Delmas, D., Huret, M., Herbland, A., 2005. Satellite-derived parameters for biological modelling in coastal waters: illustration over the eastern continental shelf of the Bay of Biscay. Remote Sens. Environ. 95 (1), 29—46.

Grunwald, M., Dellwig, O., Liebezeit, G., Schnetger, B., Reuter, R., Brumsack, H., 2007. A novel time-series station in the Wadden Sea (NW Germany): first results on continuous nutrient and methane measurements. Mar. Chem. 107 (3), 411—421.

Hall, P., Hulth, S., Hulthe, G., Landen, A., Tengberg, A., 1996. Benthic nutrient fluxes on a basin-wide scale in the Skagerrak (north-eastern North Sea). J. Sea Res. 35 (1—3), 123—137.

Henderson, E.W., Steele, J.H., 1993. Problems in the meso-scale interpretation of satellite chlorophyll data. Cont. Shelf Res. 13 (8—9), 845—861.

Joint, I., Pomroy, A., 1993. Phytoplankton biomass and production in the southern North Sea. Mar. Ecol. Progr. Ser. 99, 169—182.

Knefelkamp, B., Carstens, K., Wiltshire, K.H., 2007. Comparison of different filter types on chlorophyll-a retention and nutrient measurements. J. Exp. Mar. Biol. Ecol. 345 (1), 61—70.

Koschinsky, A., Gaye-Haake, B., Arndt, C., Maue, G., Spitzy, A., Winkler, A., Halbach, P., 2001. Experiments on the influence of sediment disturbances on the biogeochemistry of the deep-sea environment. Deep Sea Res. II 48 (17—18), 3629—3651.

Koseff, J.R., Holen, J.K., Monismith, S.G., Cloern, J.E., 1993. Coupled effects of vertical mixing and benthic grazing on phytoplankton populations in shallow, turbid estuaries. J. Mar. Res. 51 (4), 843—868.

Loebl, M., Colijn, F., van Beusekom, J., 2008. Increasing nitrogen limitation during summer in the list tidal basin (northern Wadden Sea). Helgol. Mar. Res. 62 (1), 59—65.

Loebl, M., Colijn, F., van Beusekom, J., Baretta-Bekker, J., Lancelot, C., Philippart, C., Rousseau, V., Wiltshire, K., 2009. Recent patterns in potential phytoplankton limitation along the Northwest European continental coast. J. Sea Res. 61 (1—2), 34—43.

Lou, J., Schwab, D., Beletsky, D., Hawley, N., 2000. A model of sediment resuspension and transport dynamics in southern Lake Michigan. J. Geophys. Res. 105 (C3), 6591—6610.

Lucas, L., Cloern, J., Koseff, J., Monismith, S., Thompson, J., 1998. Does the Sverdrup critical depth model explain bloom dynamics in estuaries? J. Mar. Res. 56 (2), 375—415.

Lucas, L.V., Koseff, J.R., Cloern, J.E., Monismith, S.G., Thompson, J.K., 1999. Processes governing phytoplankton blooms in estuaries: I. The local production-loss balance. Mar. Ecol. Progr. Ser. 187, 1—15.

Malone, T., Falkowski, P., Hopkins, T., Rowe, G., Whitledge, T., 1983. Mesoscale response of diatom populations to a wind event in the plume of the Hudson River. Deep Sea Res. Part A: Oceanogr. Res. Pap. 30 (2), 149—170.

May, C., Koseff, J., Lucas, L., Cloern, J., Schoellhamer, D., 2003. Effects of spatial and temporal variability of turbidity on phytoplankton blooms. Mar. Ecol. Progr. Ser. 254, 111—128.

Mei, Z.P., Saucier, F.J., Le Fouest, V., Zakardjian, B., Sennville, S., Xie, H., Starr, M., 2010. Modelling the timing of spring phytoplankton bloom and biological production of the Gulf of St. Lawrence (Canada): effects of coloured dissolved organic matter and temperature. Cont. Shelf Res. 30 (19), 2027–2042.

Moll, A., 1998. Regional distribution of primary production in the North Sea simulated by a three-dimensional model. J. Mar. Syst. 16 (1–2), 151–170.

Morel, A., Prieur, L., 1977. Analysis of variations in ocean colour. Limnol. Oceanogr. 22, 709–722.

Müller, D., 2010. Geostatistische analyse der Chlorophyllverteilung in der Nordsee basierend auf MERIS-satellitendaten. University of Hamburg (Ph.D. thesis).

Müller, D., Krasemann, H., Brewin, R.J., Brockmann, C., Deschamps, P.-Y., Doerffer, R., Fomferra, N., Franz, B.A., Grant, M.G., Groom, S.B., et al., 2015. The ocean colour climate change initiative: I. A methodology for assessing atmospheric correction processors based on in-situ measurements. Remote Sens. Environ. 162, 242–256.

Onken, R., Riethmüller, R., 2010. Determination of the freshwater budget of tidal flats from measurements near a tidal inlet. Cont. Shelf Res. 30 (8), 924–933.

Petersen, W., Wehde, H., Krasemann, H., Colijn, F., Schroeder, F., 2008. Ferrybox and MERIS — assessment of coastal and shelf sea ecosystems by combining in-situ and remotely sensed data. Estuar. Coast. Shelf Sci 77, 296–307.

Pietrzak, J.D., de Boer, G.J., Eleveld, M.A., 2011. Mechanisms controlling the intra-annual mesoscale variability of SST and SPM in the southern North Sea. Cont. Shelf Res. 31 (6), 594–610.

Radach, G., Berg, J., Hagmeier, E., 1990. Long-term changes of the annual cycles of meteorological, hydrographic, nutrient and phytoplankton time series at Helgoland and at LV Elbe 1 in the German Bight. Cont. Shelf Res. 10 (4), 305–328.

Renz, J., Mengedoht, D., Hirche, H., 2008. Reproduction, growth and secondary production of Pseudocalanus elongatus Boeck (Copepoda, Calanoida) in the southern North Sea. J. Plankton Res. 30 (5), 511–528.

Roden, C.M., 1994. Chlorophyll blooms and the spring/neap tidal cycle: observations at two stations on the coast of Connemara, Ireland. Mar. Biol. 118 (2), 209–213.

Sharples, J., 2008. Potential impacts of the spring-neap tidal cycle on shelf sea primary production. J. Plankton Res. 30 (2), 183–197.

Sharples, J., Ross, O.N., Scott, B., Greenstreet, S., Fraser, H., 2006. Inter-annual variability in the timing of stratification and the spring bloom in the north-western North Sea. Cont. Shelf Res. 26 (6), 733–751.

Simpson, J., Brown, J., Matthews, J., Allen, G., 1990. Tidal straining, density currents, and stirring in the control of estuarine stratification. Estuar. Coasts 13 (2), 125–132.

Sloth, N., Riemann, B., Nielsen, L., Blackburn, T., 1996. Resilience of pelagic and benthic microbial communities to sediment resuspension in a coastal ecosystem, Knebel Vig, Denmark. Estuar. Coast. Shelf Sci. 42 (4), 405–415.

Soetaert, K., Herman, P., Kromkamp, J., 1994. Living in the twilight: estimating net phytoplankton growth in the Westerschelde estuary (The Netherlands) by means of an ecosystem model (MOSES). J. Plankton Res. 16 (10), 1277–1301.

Sournia, A., Birrien, J.L., Douville, J.L., Klein, B., Viollier, M., 1987. A daily study of the diatom spring bloom at Roscoff (France) in 1985: I. The spring bloom within the annual cycle. Estuar. Coast. Shelf Sci. 25 (3), 355–367.

Stanev, E., Brink-Spalink, G., Wolff, J., 2007. Sediment dynamics in tidally dominated environments controlled by transport and turbulence: a case study for the east Frisian Wadden Sea. J. Geophys. Res. O 112 (C4), c04018.

Staneva, J., Stanev, E., Wolff, J.-O., Badewien, T., Reuter, R., Flemming, B., Bartholomä, A., Bolding, K., 2009. Hydrodynamics and sediment dynamics in the German Bight: a focus on observations and numerical modelling in the east Frisian Wadden Sea. Cont. Shelf Res. 29 (1), 302–319.

Stoeck, T., Kroncke, I., 2001. Influence of particle mixing on vertical profiles of chlorophyll A and bacterial biomass in sediments of the German Bight, Oyster Ground, and Dogger Bank (North Sea). Estuar. Coast. Shelf Sci. 52 (6), 783–795.

von Storch, H., Zwiers, F.W., 2001. Statistical Analysis in Climate Research. Cambridge University Press.

Sündermann, J., Hesse, K., Beddig, S., 1999. Coastal mass and energy fluxes in the south-eastern North Sea. Ocean Dyn. 51 (2), 113–132.

Tengberg, A., Almroth, E., Hall, P., 2003. Resuspension and its effects on organic carbon recycling and nutrient exchange in coastal sediments: in-situ measurements using new experimental technology. J. Exp. Mar. Biol. Ecol. 285, 119–142.

Tian, T., Merico, A., Su, J., Staneva, J., Wiltshire, K., Wirtz, K., 2009. Importance of resuspended sediment dynamics for the phytoplankton spring bloom in a coastal marine ecosystem. J. Sea Res. 62 (4), 214–228.

Tian, T., Su, J., Flöser, G., Wiltshire, K., Wirtz, K., 2011. Factors controlling the onset of spring blooms in the German Bight 2002–2005: light, wind, and stratification. Cont. Shelf Res. 31 (10), 1140–1148.

Wainright, S., 1990. Sediment-to-water fluxes of particulate material and microbes by resuspension and their contribution to the planktonic food web. Mar. Ecol. Progr. Ser. 62 (3), 271–281.

Wild-Allen, K., Lane, A., Tett, P., 2002. Phytoplankton, sediment and optical observations in Netherlands coastal water in spring. J. Sea Res. 47 (3–4), 303–315.

Wiltshire, K., Malzahn, A., Wirtz, K., Greve, W., Janisch, S., Mangelsdorf, P., Manly, B., Boersma, M., 2008. Resilience of North Sea phytoplankton spring bloom dynamics: an analysis of long-term data at Helgoland roads. Limnol. Oceanogr. 53 (4), 1294–1302.

Wirtz, K., Pahlow, M., 2010. Dynamic CHL and N–C regulation in algae optimizes instantaneous growth rate. Mar. Ecol. Progr. Ser. 402, 81–96.

Ziervogel, K., Bohling, B., 2003. Sedimentological parameters and erosion behaviour of submarine coastal sediments in the south-western Baltic Sea. Geo-Mar. Lett. 23 (1), 43–52.